• Basic Research •

Developmental properties of parvalbumin-positive gamma-aminobutyric acid interneurons and the effect of fluoxetine treatment and binocular form deprivation on them in the visual cortex of adult rats

Qiao-Yun Wang^{1,2}, Tao-Tao Xu³, Xing-Hao Wen⁴, Man-Hui Zhu¹, Gao-Yu Shen¹, Yi-Qian Xu¹, Yang Guo¹, Lai-Qing Xie^{1,5}, Xiao-Yan Ji¹

¹Department of Ophthalmology, the Second Affiliated Hospital of Soochow University, Suzhou 215004, Jiangsu Province, China

²Department of Ophthalmology, Kunshan Hospital of Traditional Chinese Medicine, Affiliated Hospital of Nanjing University of Chinese Medicine, Suzhou 215300, Jiangsu Province, China

³Department of Ophthalmology, Kunshan First People's Hospital Affiliated to Jiangsu University, Suzhou 215300, Jiangsu Province, China

⁴Suzhou Medical College of Soochow University, Suzhou 215123, Jiangsu Province, China

⁵State Key Laboratory of Radiation Medicine and Protection, Soochow University, Suzhou 215000, Jiangsu Province, China **Co-first Authors:** Qiao-Yun Wang and Tao-Tao Xu

Correspondence to: Xiao-Yan Ji. Department of Ophthalmology, the Second Affiliated Hospital of Soochow University, Suzhou 215004, Jiangsu Province, China. suzhoujixiaoyan@163.com; Lai-Qing Xie. Department of Ophthalmology, the Second Affiliated Hospital of Soochow University, Suzhou 215004; State Key Laboratory of Radiation Medicine and Protection, Soochow University, Suzhou 215000, Jiangsu Province, China. xielaiqing@suda.edu.cn Received: 2024-12-28 Accepted: 2025-07-28

Abstract

- AIM: To investigate the postnatal development of parvalbumin (PV)-positive gamma-aminobutyric acid (GABA) interneurons and the co-expression of perineuronal nets (PNNs) and PV in the visual cortex of rats, as well as the regulatory effects of fluoxetine (FLX) treatment and binocular form deprivation (BFD) on these indices.
- **METHODS:** Wistar rats were assigned to three experimental cohorts: 1) Age-related groups: postnatal week (PW) 1, PW3, PW5, PW7, and PW9; 2) FLX treatment duration groups: FLX OW, FLX 2W, FLX 4W, FLX 6W, and FLX 8W; 3) Intervention groups: control (Cont), FLX, BFD,

and BFD+FLX. The levels of PNNs, PV, and PNNs/PV coexpression in the visual cortex were detected and analyzed.

- **RESULTS:** The density of PV-positive cells and the coexpression of PNNs and PV increased gradually with the maturation of the visual cortex (b=0.960, P<0.01). The ratio of PV-positive cells surrounded by PNNs to total PV-positive cells (PNNs⁺/PV⁺/total PV⁺) was significantly decreased in the FLX 4W group (χ^2 =9.03, P=0.003). There was no significant difference in the PNNs⁺/PV⁺/total PV⁺ ratio between the FLX and BFD groups (χ^2 =1.08, P=0.161), but a significant difference was observed between the BFD+FLX group and the BFD group (χ^2 =5.82, P<0.01).
- **CONCLUSION:** The number of PV-positive neurons and PNNs-surrounded PV neurons in the rat visual cortex increases postnatally and reaches adult levels by postnatal week 7. Chronic FLX treatment downregulates these expressions. Combined 4-week FLX treatment and BFD exerts a more significant inhibitory effect on the PNNs⁺/PV⁺/ total PV⁺ ratio than either intervention alone.
- **KEYWORDS:** parvalbumin; gamma-aminobutyric acid; perineuronal nets; fluoxetine; visual cortex plasticity

DOI:10.18240/ijo.2025.12.03

Citation: Wang QY, Xu TT, Wen XH, Zhu MH, Shen GY, Xu YQ, Guo Y, Xie LQ, Ji XY. Developmental properties of parvalbumin-positive gamma-aminobutyric acid interneurons and the effect of fluoxetine treatment and binocular form deprivation on them in the visual cortex of adult rats. *Int J Ophthalmol* 2025;18(12):2237-2245

INTRODUCTION

In the early critical period (CP) of visual development, glutamate neurotransmitters dominate visual circuit formation, whereas the number of gamma-aminobutyric acid (GABA) neurotransmitters gradually increases in the later CP. The balance between excitatory and inhibitory neurons governs the "opening" and "closing" of the CP in visual development^[1-2], which is also the biological basis for the reactivation of ocular

dominance (OD) plasticity in adult animals^[3]. Neurons with the Ca²⁺-binding protein parvalbumin (PV), neuropeptide somatostatin, and ionotropic 5-hydroxytryptamine receptor are the three primary subtypes of GABA interneurons. These constitute 40% of all GABA neurons and most frequently regulate CP plasticity^[4-5]. Previous studies have shown that PV expression aligned with the onset and closure of CP and was promoted by brain-derived neurotrophic factor^[6]. The elimination of fast-spiking potassium currents in PVpositive neurons could significantly reduce OD plasticity^[7]. Perineuronal nets (PNNs) are important central nervous system (CNS) extracellular matrix components that form networks around particular neurons and their connections^[8-9]. They modulate synaptic development, especially surrounding PVpositive inhibitory interneurons^[10]. The cortical expression of PNNs is low during CP and higher in a latter period. They function as a "structural break" in the visual cortex synaptic plasticity[11-12]. PNNs surround mature CNS GABA neurons. The degradation of PNNs decreases GABA neuron inhibition in the visual cortex, and then restoring terminated cortical plasticity in adulthood^[13]. Given the critical roles of GABA interneurons, PV-positive neurons, and PNNs during visual plasticity, we proposed a preliminary investigation of the following: 1) the development of PV-positive neurons and how their co-expression with PNNs changes; 2) how fluoxetine (FLX) treatment for different durations affects PV-positive neurons and their co-expression with PNNs in adult rats; and 3) how FLX treatment and binocular form deprivation (BFD) modify PV-positive neurons and their co-expression with PNNs in adult rats and reverse visual cortical plasticity. In this study, we sought to understand the link between the expression of PV-positive GABA neurons and visual experience, the role of PPNs/PV in reversing adult visual cortex plasticity, and the underlying mechanisms, aiming to identify novel drug targets for treating adult amblyopia.

PARTICIPANTS AND METHODS

Ethical Approval The study followed the ethical principles of the Declaration of Helsinki and all animal experimental procedures were approved by the Committee on the Ethics of Animal Experiments of Soochow University, approval number (SLER 2022120). The ARVO statement was followed in the treatment of all animals.

Study of Developmental Changes in PV-positive Neurons and PNNs/PV Co-expression Forty clean-grade, healthy Wistar rats of both sexes were used. The rats were separated into five groups based on the postnatal weeks (PW): PW1 (1 week old), PW3 (3 weeks old), PW5 (5 weeks old), PW7 (7 weeks old), and PW9 (9 weeks old). Each group had eight rats. Effect of FLX Administration for Different Durations on PV-positive Neurons and PPNs/PV Co-expression in Adult

Rats Forty 10-week-old (PW10) clean-grade Wistar rats, both males and females, were used. They were divided into five groups randomly: a control group (administered normal water) and four FLX groups (administered 0.2 mg/mL FLX in water for 2, 4, 6, or 8wk). Each group had eight rats.

Study of the Effects of FLX and BFD on PNNs and PV in the Visual Cortex of Adult Rats We used 32 clean-grade Wistar rats at PW10, both male and female. They were divided into four groups: the control group (administered normal water), the FLX group (treated with 0.2 mg/mL FLX in water for 4wk), the BFD group (subjected to 2wk of BFD with normal water), and the FLX+BFD group (treated with 0.2 mg/mL FLX in water for 4wk and subjected to BFD for 2wk). Each group had eight rats. The animals were provided by the Experimental Animal Centre, School of Pharmacology, Soochow University (approval number: SLER 2022120). The animals were housed in a well-ventilated space under a temperature range of 18°C to 25°C, relative humidity of 40% to 70%, and 12h of light exposure each day and night.

Binocular Form Deprivation Modeling Ten percent chloral hydrate dissolved in 0.3 mL/100 g intraperitoneally sedated rats. Iodophor was used to clean the eyelids, and the hair around both lid edges was trimmed. After the skin and lid tissue were cut (1.0 mm from the upper and lower lid margins), the eyes were closed with 6-8 interrupted 5-0 silk stitches and treated with gentamycin ointment to avoid infection. The rats were housed normally, kept warm, and monitored until they woke up. The suture sites were observed daily, and the rats with lid dehiscence or corneal damage sutures were removed from the experiment, which were replaced with spare rats with the same treatment.

Main Reagents and Instruments The following reagents and instruments were purchased: rabbit anti-rat parvalbumin antibody (Abcam, ab64555, USA); mouse anti-rat glyceraldehyde-3-phosphate dehydrogenase (GADPH) primary antibody (Shanghai Kangcheng), lectin from *Wisteria Floribunda* agglutinin (WFA, Sigma, L8258, USA), Cy3-labeled goat anti-rabbit secondary antibody, alkaline phosphatase-labeled goat anti-rabbit secondary antibody (Santa Cruz, USA), Streptavidin-Alexa Fluor (R&D, item no.4800-30-14), polyvinylidene fluoride (PVDF) membrane (Roche, Germany), vertical plate electrophoresis tank (Bio-Rad, USA), A-5082 digital display enzyme marker (Sunrise, Australia), laser confocal microscope (Leica, Germany).

Immunofluorescence Histochemistry The rats were routinely anesthetized. The left ventricle was flushed with 0.01 mol/L phosphate buffer saline (PBS) and fixed with 4% paraformaldehyde perfusion. The brain tissues were removed, and the occipital lobe was isolated and fixed overnight at 4°C. The tissues were then transferred to 30% sucrose solution for

dehydration. The rat brain stereotaxic atlas was used to select the optic cortex tissue. Serial frozen sections (20 μm) were cut along the coronal plane. PBS was used as the negative control. The tissues were treated overnight with goat serum for 1h with PV primary antibody (1:100) and WFA (1:200) in a wet box at 4°C. PBS was added after 2h of treatment at 25°C with Cy3-labeled goat anti-rabbit secondary antibody (1:500) and Streptavidin-Alexa Fluor (1:200). The tissues were washed with PBS, blocked with 50% glycerol, and immediately examined using a laser confocal microscope. Image-Pro plus 4.5 software was used to count positive cells in two 250 $\mu m \times 250~\mu m$ optic cortex IV regions.

Western Blotting Analysis Brain tissues were rapidly removed

from anesthetized rats and stored at -70°C. Brain tissues from the occipital pole 1.5-3 mm anterior to the visual cortex were cut into 200 µm serial frozen sections at low temperature. Gray matter was manually excised using the stereotaxic atlas of the rat brain, rapidly placed in a lysate, homogenized on ice, and centrifuged at 12 000 r/min for 5min at 4°C. The supernatant was stored at -20°C. Total visual cortex protein (100 μg) was denatured by treating at 100°C for 10min. This was followed by polyacrylamide gel electrophoresis, PVDF membrane electrotransfer, and 2h of treatment with tris-buffered saline with tween 20 (TBST) and 5% bovine serum albumin solution (BSA). Next, the proteins were treated overnight with PV and GADPH primary antibodies (1:500) at 4°C. The membrane was colored with 5-bromo-4-chloro-3-indolyl phosphate/nitro blue tetrazolium (BCIP/NBT) after treatment with alkaline phosphatase-labeled goat anti-rabbit and anti-mouse secondary antibodies for 1h at 37°C. The transfer film was subjected to thin-layer densitometry. Quantity One Version 4.4 was used to calculate the integrated optical density (IOD) of each band. each group of protein samples were taken from two rats and the experiment was repeated for 5 times. Statistical Analysis Statistical analysis was performed using SPSS 25.0 with a significant threshold of 0.05. The data were expressed in terms of mean±standard deviation (SD) and exhibited normal distribution according to the W-test. Depending on variance homogeneity, we used ANOVA or the Kruskal-Wallis tests to evaluate the number of PNNs and PVpositive cells and PV expression in the groups. We adjusted for multiple comparisons using the Bonferroni method; the significance level was 0.05 divided by the number of comparisons. Using simple linear regression, we examined temporal changes in PNNs and PV-positive cell counts and PV expression. Chi-square test was used to compare the number of

RESULTS

Developmental Changes in PV-positive Neurons and PNNs/PV Co-expression in the Visual Cortex of Rats

PV-positive cells surrounded by PNNs to total PV-positive cells.

We used WFA to label the N-acetylgalactosamine residues of chondroitin sulfate proteoglycans (CSPGs), which is the conventional method for detecting PNNs. We analyzed the variations in the expression of the residues in rat visual cortex development. PNNs encapsulated few visual cortex neurons in the PW1 group, but at PW3, the number increased significantly (t=12.31, P=0.010; PW3 vs PW1) and was higher in the PW5 group than in the PW3 group (t=10.31, P=0.014; PW5 vs PW3). The number of neurons surrounded by PNNs was the highest at PW9 (220.13±10.34/mm²; Figures 1 and 2). PV-positive cells in the visual cortex of rats appeared in the PW3 group. The number of cells increased in the PW5 group (t=9.01, P=0.004; PW5 vs PW3) and peaked in the PW9 group (158.72±11.22/mm²). A gradual increase was observed from PW3 to PW7 (standardized regression coefficient b=0.850, P<0.05); no statistically significant difference was observed between the PW9 and PW7 groups (t=3.12, P=0.072; PW9 versus PW7; Figures 1A, 2). PV-positive expression signals were observed in both the cell membrane and the cytoplasm. The majority of PV-positive neurons were encapsulated by PNNs, the most significant subtype of GABA interneurons (Figure 2). The abundance of PV indicates the development of inhibitory interneurons, in the same manner as the number of PNNs indicates the maturation of neurons in the visual cortex. The number of PV-positive cells surrounded by PNNs increased gradually with the development of the visual cortex (standardized regression coefficient b=0.960, P<0.01). PV was rarely expressed in rats in the PW1 group, but the proportion of PV-positive cells surrounded by PNNs to total PV-positive cells (PNNs⁺/PV⁺/total PV⁺) in the brain of rats in the PW3 group was 21.26%±6.73%, whereas this proportion was 40.29%±8.23%, 77.80%±11.43%, and 80.70%±15.19% in the PW5, PW7, and PW9 groups, respectively. The group difference was statistically significant ($\chi^2 = 10.26$, P = 0.001; Figure 1B). PV expression increased gradually during the postnatal weeks, nearing adult levels in the PW7 group (Z=1.73, P=0.492, PW7 vs PW9; Figure 3).

Effect of FLX Treatment on PV-positive Neurons and PPNs/PV Co-expression in the Visual Cortex of Adult rats. The number of PNNs-positive cells in the visual cortex of adult rats (at PW10) was approximately $227.22\pm17.61/\text{mm}^2$, and the number of PV-positive cells was approximately $169.72\pm15.16/\text{mm}^2$. FLX feeding significantly reduced the number of PNNs and PV-positive cells (Figure 4); the density of PNNs-positive neurons in the visual cortex decreased gradually as the duration of FLX treatment increased (standardized regression coefficient b=-0.973, P<0.01). The density of PV-positive cells decreased gradually (standardized regression coefficient b=-0.959, P<0.05; Figure 4A). The number of PV-positive cells surrounded by PNNs decreased

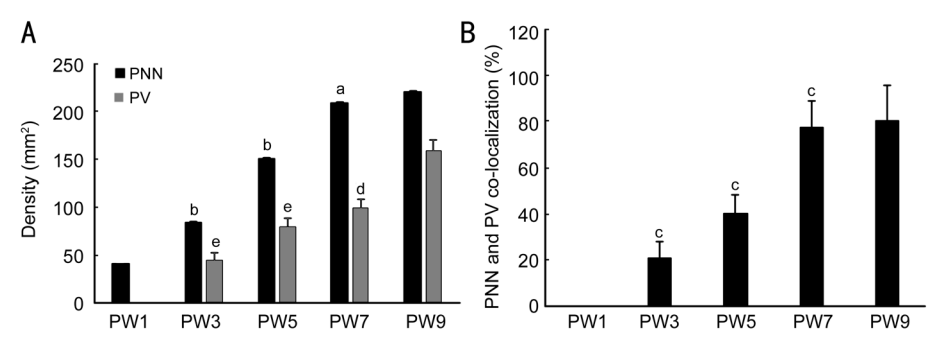


Figure 1 Changes in PNNs and PV-positive cell densities and PNNs/PV co-expression in the visual cortex of rats at different postnatal weeks A: The expression of PNNs and density of PV-positive cells in the visual cortex of rats at 1, 3, 5, 7, and 9wk after birth; B: Changes in the proportion of PV-positive cells surrounded by PNNs to total PV-positive cells in each group (%). PNNs: Perineuronal nets; PV: Parvalbumin; PW: Postnatal weeks. Comparison between adjacent groups, ^aP<0.05, ^bP<0.01, ^cP<0.001, ^cP<0.001.

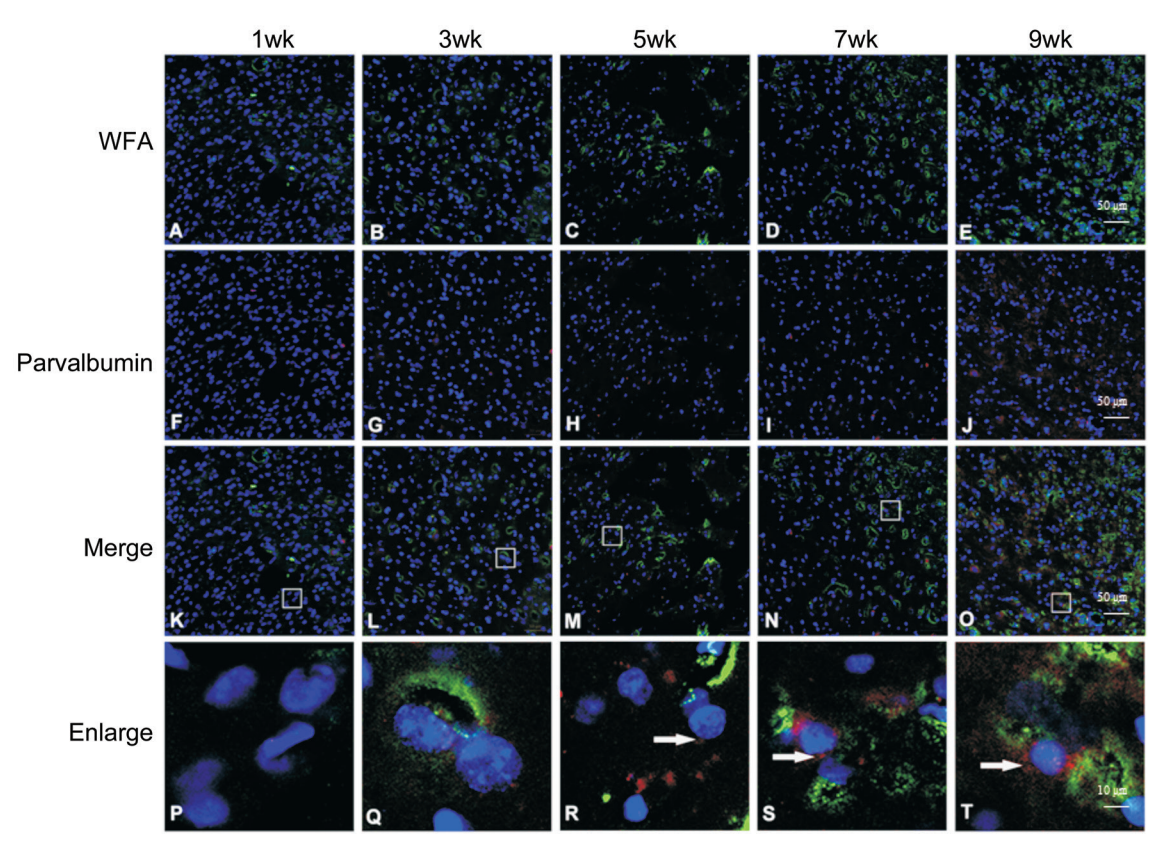


Figure 2 Developmental changes in PNNs (WFA-labeled) and PV expression in the visual cortex of rats observed by immunofluorescent histochemical staining, magnification 200× A-E: Images of PNNs (green fluorescence) after fluorescent staining at 1, 3, 5, 7, and 9wk; F-J: Images of PV (red fluorescence) after fluorescent staining at weeks 1, 3, 5, 7, and 9; K-O: Images of PNNs and PV co-staining; Blue fluorescence from DAPI staining (nucleus); P-T: Partially enlarged images (within the box) in Figures K-O (white arrow points to PV). A-O: Magnification 200×, scale 50 μm; P-T: Magnification 1000×, scale 10 μm. PNNs: Perineuronal nets; PV: Parvalbumin; WFA: Wisteria floribunda agglutinin.

gradually as the duration of administration increased (standardized regression coefficient b=-0.920, P<0.01), but the PNNs $^+$ /PV $^+$ /total PV $^+$ level did not change significantly at 2wk of FLX administration (χ^2 =1.69, P=0.138; FLX 2W vs Cont). The PNNs $^+$ /PV $^+$ /total PV $^+$ value decreased significantly at 4wk of FLX administration (χ^2 =9.03, P=0.003; FLX 4W vs FLX 2W). When the number of weeks of feeding increased again, the PNNs $^+$ /PV $^+$ /total PV $^+$ value did not change significantly (χ^2 =1.47, P=0.386, FLX 6W vs FLX 4W; χ^2 =0.86, P=0.419, FLX 8W vs FLX 4W; Figures 4B, 5).

Changes in the Density of PV-positive Neurons and PNNs/PV Co-expression After FLX- and BFD-induced Activation of Plasticity in the Visual Cortex of Adult Rats FLX and BFD promote visual cortical plasticity in adult rats^[14]. In this study, we discovered PV-positive neurons and PPNs/PV co-expression in the visual cortex of healthy adult (PW10) rats following 4wk of treatment with 0.2 mg/mL FLX in water, 2wk of BFD, and 2wk of BFD+FLX. The number of PV-positive neurons differed significantly between groups (*F*=21.321, *P*=0.008); a two-by-two comparison of the FLX,

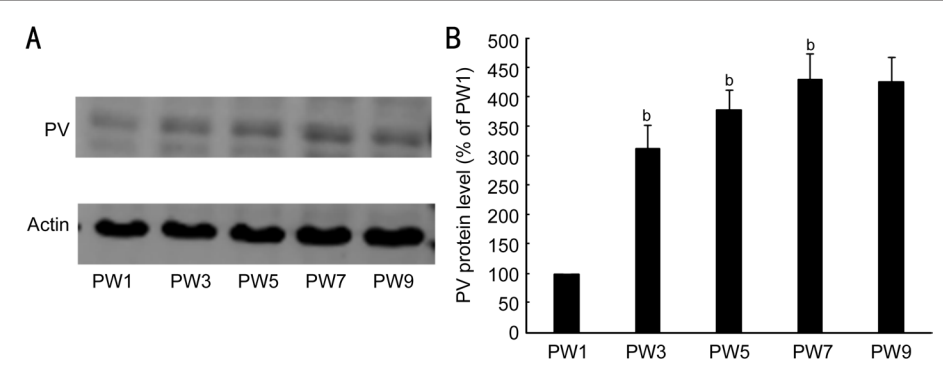


Figure 3 Expression of PV in the visual cortex of rats at different postnatal weeks by western blotting A: The expression of PV in the visual cortex of rats at 1, 3, 5, 7, and 9wk after birth. Actin was used as the internal control; B: Expression intensity (%) of PV in each group relative to that at PW1. PV: Parvalbumin; PW: Postnatal weeks. Comparison between adjacent groups, ^bP<0.01.

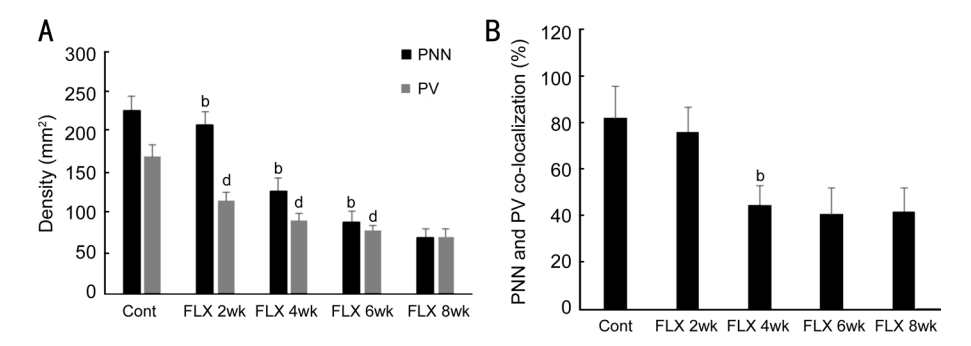


Figure 4 Effect of FLX treatment for varying durations on the density of PNNs and PV-positive cells and PNNs/PV co-expression in the visual cortex of adult rats A: The density of PNNs and PV-positive cells in adult rats at 0, 2, 4, 6 and 8wk of FLX feeding; B: The proportion of PV-positive cells surrounded by PNNs to the total number of PV-positive cells in each group (%). PNNs: Perineuronal nets; PV: Parvalbumin; PW: Postnatal weeks. Comparison between adjacent groups, ^bP<0.01, ^dP<0.05.

BFD, and BFD+FLX groups with the control group showed a significantly lower number of PV-positive neurons (*t*=13.06, 10.68, 10.11; *P*<0.017); the density of PNNs-positive cells differed significantly between groups (F=13.014, P=0.026), and the FLX, BFD, and BFD+FLX groups also showed a significantly lower density than the Cont group (t=8.46, 8.42, 13.13; *P*<0.017; Figure 6A, Figure 7). A statistically significant difference was observed in the intensity of PV expression between the groups (H=6.603, P<0.05; Figure 8). The PNNs⁺/ PV⁺/total PV⁺ value differed significantly between groups, and this value also reduced significantly in the FLX, BFD, and BFD+FLX groups compared to that in the Cont group $(\chi^2=13.49, 13.88, 16.10; P<0.01)$. No statistically significant difference was observed between the FLX and BFD groups $(\chi^2=1.08, P=0.161)$. The values in the BFD+FLX and BFD groups showed a statistically significant difference (χ^2 =5.82, P<0.01). The above data demonstrated that, when it came to reducing the number of PNNs⁺/PV⁺/total PV⁺ cells, FLX treatment combined with BFD exerted an effect that was different from the effect of FLX treatment or BFD alone (Figure 6B).

DISCUSSION

PNNs are network-like structures surrounding specific neurons and synapses in the CNS. CSPGs, hyaluronic acid, connexins,

and tendon glycoprotein-R constitute the neurocentral extracellular interstitium and regulate visual plasticity. Our findings showed that PNNs expression in the visual cortex is visual experience-dependent, with low expression observed during the CP and usual expression levels after the CP, thus indicating that the level of PNNs can indicate neurological maturation^[15-16]. WFA is a lectin protein with a biotin identifier on one end that selectively binds to the end of N-acetylgalactosamine residues of CSPGs^[17]. Streptavidin binds to the biotin marker on one end and to fluorescein isothiocyanate on the other, changing the colors of CSPGs and indicating the level of PNNs^[18]. The WFA agglutination reaction is the gold standard for identifying CS subtypes in PNNs in the CNS^[19]. In this study, immunofluorescence and protein gel electrophoresis were used to examine how PVpositive GABA interneurons develop and function alongside PNNs. The following conclusions were drawn: PV-positive neurons were expressed in the visual cortex in a visual experience-dependent manner, gradually increasing with visual development and stabilizing by the end of adulthood. The majority of PV-positive neurons, as the most important subtype of GABA interneurons, were encapsulated by PNNs; the number of PV-positive cells encapsulated by PNNs increased with the gradual development of the rat visual cortex, reaching

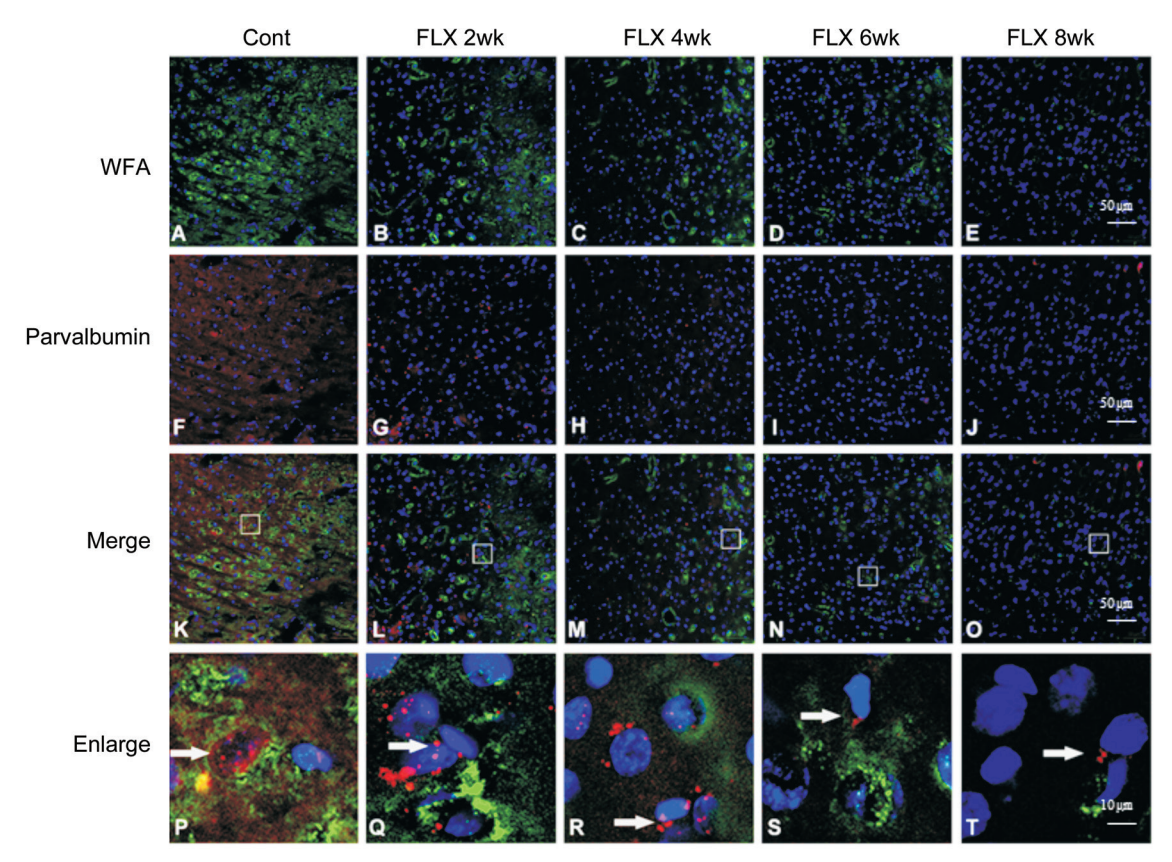


Figure 5 Effect of the duration of FLX administration on PNNs and PV expression in the visual cortex of adult rats by immunofluorescence histochemical staining; magnification 200× A-E: Images of PNNs (WFA-labeled, green fluorescence) after fluorescent staining at 0, 2, 4, 6, and 8wk of FLX feeding; F-J: PV detection by fluorescent staining (red fluorescence) at 0, 2, 4, 6, and 8wk of FLX feeding; K-O: Images of PNNs and PV co-staining; blue fluorescence from DAPI staining (nucleus); P-T: Partially enlarged images of Figures (within the box) K-O (white arrow points to PV). A-O: Magnification 200×, scale 50 μm; P-T: Magnification 1000×, scale 10 μm. PV: Parvalbumin; PNNs: Perineuronal nets; WFA: *Wisteria floribunda* agglutinin.

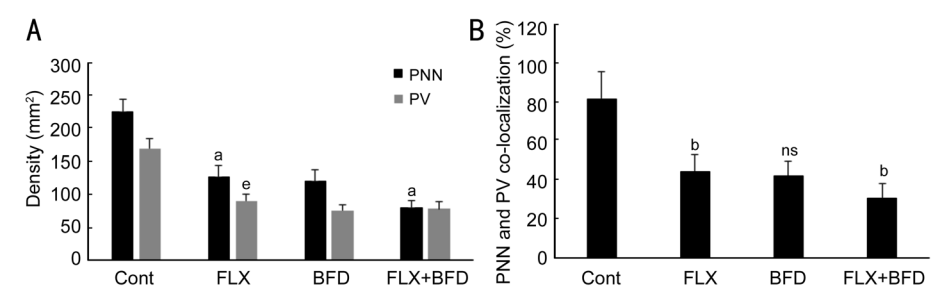


Figure 6 Density of PNNs- and PV-expressing cells and PNNs and PV co-expression in the visual cortex of adult rats under different treatment conditions A: The density of PNNs and PV-positive cells in each group; B: The proportion of PV-positive cells surrounded by PNNs to total PV-positive cells in each group. Cont: control; FLX: fluoxetine; BFD: binocular form deprivation; PNNs: Perineuronal nets; PV: Parvalbumin. Comparison between adjacent groups, ^aP<0.05, ^bP<0.01, ^eP<0.01, ns: No statistical significance.

usual expression levels by the end of the CP (7wk after birth). The usual perspective is that the level of PNNs reflects neuron maturation, and PV is the primary subtype of inhibitory GABA neurons. Thus, we hypothesized that the PNNs $^+$ /PV $^+$ /total PV $^+$ level can reflect GABA neuron maturation. The PNNs $^+$ /PV $^+$ /total PV $^+$ level increased from a lower level at the onset of plasticity (21.26% \pm 6.73%) to a higher level in adulthood (80.70% \pm 15.19%), predicting the maturation of GABA interneurons and providing a structural basis for the closure of GABA interneurons controlling plasticity, according to our

findings. Synaptic plasticity was inhibited and visual cortex plasticity was suppressed because GABA interneurons were surrounded by dense PNNs. PV-positive, neuropeptide growth inhibitor-positive, and 5HT3a-positive GABA interneurons are the three major subtypes of GABA interneurons. PV-positive GABA interneurons are the most significant subtype participating in plasticity regulation in the visual cortex. PNNs were largely detected in PV-positive neurons and were absent in the other two subtypes in the frontal cortex and hippocampus, implying that PNNs and PV-positive

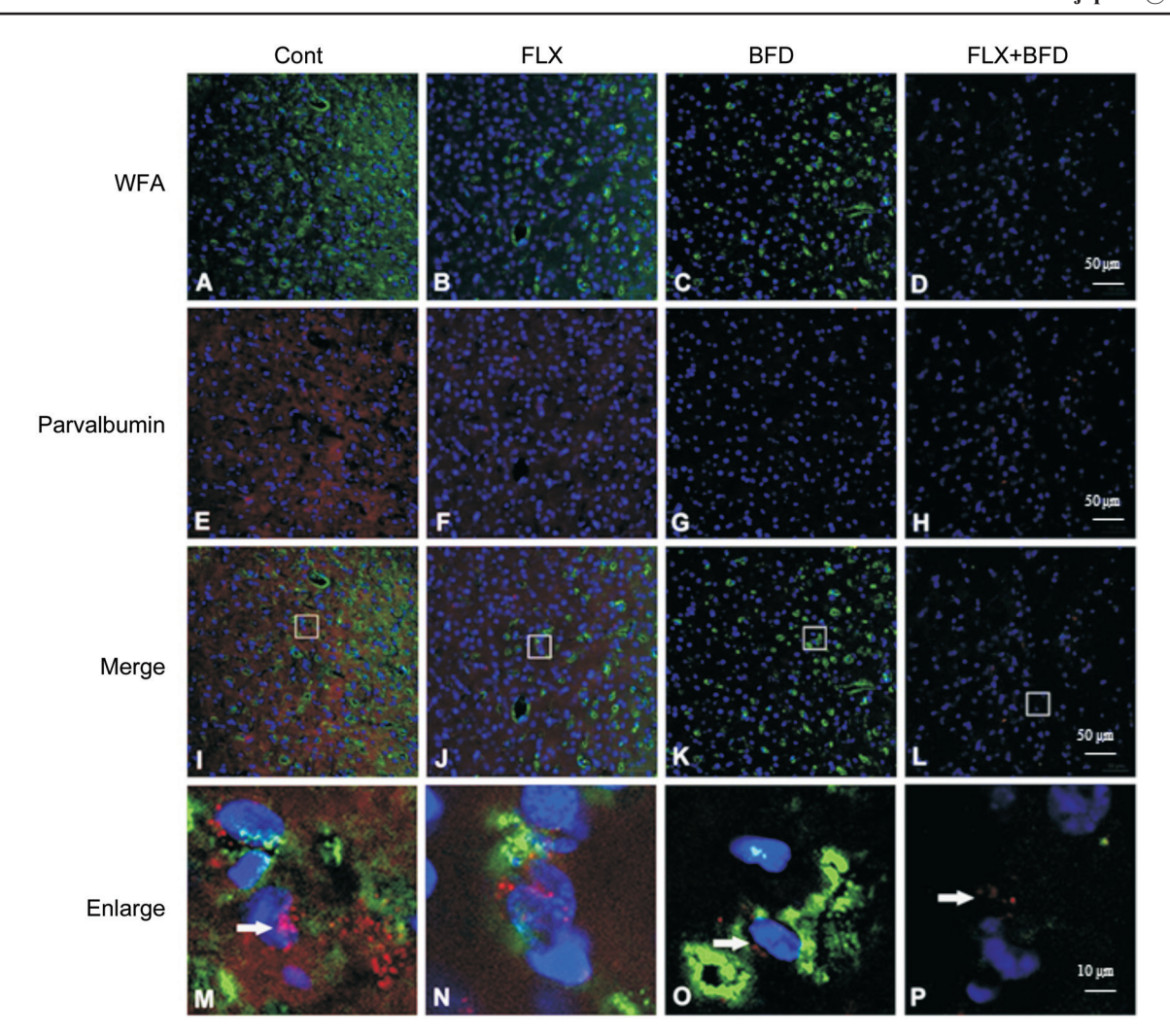


Figure 7 Immunofluorescence histochemical staining of PNNs and PV in the visual cortex of adult rats under different treatment conditions; magnification 200× A-D: Fluorescence staining of PNNs (green fluorescence) in Cont, FLX, BFD, and FLX+BFD groups, respectively; E-H: Fluorescence staining images of PV (red fluorescence) in the Cont, FLX, BFD, and FLX+BFD groups; I-L: Images of PNNs and PV co-staining; blue fluorescence from DAPI staining (nucleus); M-P: Partially magnified images of Figures (within the box) I-L (white arrow points to PV). A-L: Magnification 200×, scale 50 μm; M-P: Magnification 1000×, scale 10 μm. PV: Parvalbumin; WFA: *Wisteria Floribunda* agglutinin; Cont group: Normal water feeding; FLX group: 0.2 mg/mL fluoxetine in water fed for 4wk; BFD group: Binocular form deprivation for 2wk; FLX+BFD group: 0.2 mg/mL FLX in water fed for 4wk combined with BFD for 2wk.

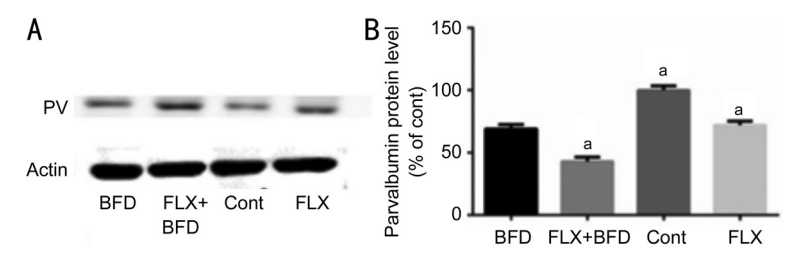


Figure 8 Western blotting of PV in the visual cortex under different treatment conditions A: Western blotting of PV in each group; actin was used as the internal control; B: Expression intensity (%) of PV in each group relative to that in the Cont group. Cont: Control; FLX: Fluoxetine; BFD: Binocular form deprivation; PV: Parvalbumin. Comparison between adjacent groups, ^aP<0.05.

GABA interneurons play a substantial role in neuroplasticity regulation^[20].

FLX, a serotonin reabsorption inhibitor, is used to treat depression. FLX has been shown to cause neuronal regeneration in mature animals^[21-23]. Adult mice treated with FLX showed juvenile traits with respect to the expression of

cell surface markers and electrophysiological properties^[24]. Besides, FLX induced the dematuration of GABA neurons in the amygdala of adult mouse^[25] and converted progenitor cells to GABA interneurons in the mouse brain^[26]. To obtain pharmacodynamic data on the effects of FLX on PV-positive neurons and PPNs/PV co-expression in the visual cortex of

adult rats, we conducted a preliminary investigation of the effects of FLX administration for varying durations on the number of PV-positive neurons and PPNs/PV co-expression in adult rats. The density of PNNs and PV-positive neurons in the visual cortex decreased as the number of weeks of FLX feeding increased. The number of PV-positive cells surrounded by PNNs reduced gradually as the number of feeding weeks increased, but the PNNs⁺/PV⁺/total PV⁺ value did not change appreciably until FLX was supplied for 4wk or longer. A longer feeding duration did not further decrease the PNNs⁺/PV⁺/total PV⁺ value. The preceding data revealed that FLX taken orally caused the optimal dematuration of the visual cortex in adult rats at 4wk. Previous research on the hippocampus and frontal cortex showed a significant increase in cortical plasticity in response to 3wk of treatment with FLX, that too administered via intraperitoneal injection rather than orally^[27]. Previous studies have reported the neurological side effects of long-term FLX administration, including one related to neuroplasticity reported by Ohira and Miyakawa^[28]. The authors discovered that an intraperitoneal injection of FLX for more than 6wk inhibited neural regeneration in the subventricular zone of adult mice. In this study, oral FLX administration for 6 and 8wk decreased the number of PNNs and PV-positive cells, but the PNNs⁺/PV⁺/total PV⁺ value did not decrease further and even increased at 8wk, indicating that long-term FLX application did not improve the dematuration of GABA neurons.

The recovery of OD plasticity in adult rats in response to 2wk of BFD has been documented previously [29-30]. BFD has practical potential as an upgrade to darkroom feeding in the treatment of adult amblyopia, but its further clinical application is limited because strict BFD is difficult to implement in humans. In this study, the BFD group served as a positive control for the FLX group, and the predictable results were obtained: FLX feeding for 4wk reduced the density of PNNs and PV-positive neurons in the visual cortex; FLX feeding for 4wk lowered the PNNs⁺/PV⁺/total PV⁺ levels, an effect that was similar to that of BFD. Our findings also showed that FLX and BFD exerted a synergistic effect in reducing PNNs⁺/ PV⁺/total PV⁺ levels, and the combined effect of the two was stronger than that of either alone. Further research is needed to determine whether this effect may be beneficial to treat adult amblyopia. FLX considerably reduced the number of PNNs in the visual cortex in this investigation. However, Ohira et al^[31] showed that the effect of FLX on PNNs varied in different cortices. FLX exerted a substantially weaker effect on PNNs in the CA3 region of the hippocampus, whereas FLX treatment at the same dose and duration exerted no significant effect on PNNs in the medial frontal cortex. A potential reason could be that the CA3 region of the hippocampus is a representative neuroplastic region with a high density of PV-positive GABA interneurons, whereas the medial frontal cortex has a low density of PV-positive GABA interneurons and does not show major changes in PNNs. This confirmed the intimate link between the number of PNNs and PV-positive GABA interneurons, emphasizing their importance in the opening and closure of synaptic plasticity.

In conclusion, FLX and BFD can maintain plasticity in the visual cortex of adult rats. The mechanism may be related to the changing quantity and function of PV-positive GABA neurons (with the decrease in inhibitory function attributed to PNNs reduction), which exhibit a significant relationship with plasticity reactivation. A more feasible approach which targets PV-positive GABA neurons could be developed to directly or indirectly lower the levels of PNNs⁺/PV⁺/total PV⁺. It may be a new focus for adult amblyopia treatment.

ACKNOWLEDGEMENTS

The authors thank Yongming Zhu PhD., for his assistance in acquiring frozen sections of the rats' optic cortex tissues and conducting the immunofluorescence histochemistry test.

Foundations: Supported by the Suzhou Science and Technology Bureau (No.SKY2023175); the Project of State Key Laboratory of Radiation Medicine and Protection; Soochow University (No.GZK1202309); the Advantage Subject Lifting Project (No.XKTJ-XK202412); the Suzhou Science and Education for Strengthening Healthcare (No. MSXM2024010); the Suzhou Medical Key Supported Disciplines (No.SZFCXK202118); the Youth Scientific Research Fund Project of Kunshan Hospital of Traditional Chinese Medicine (No.2024QNJJ06); the Postgraduate Research & Practice Innovation Program of Jiangsu Province (No.SJCX23_1673); the Undergraduate Training Program for Innovation and Entrepreneurship, Soochow University (No.202310285162Y).

Conflicts of Interest: Wang QY, None; Xu TT, None; Wen XH, None; Zhu MH, None; Shen GY, None; Xu YQ, None; Guo Y, None; Xie LQ, None; Ji XY, None.

REFERENCES

- 1 Mukerji A, Byrne KN, Yang E, *et al*. Visual cortical γ-aminobutyric acid and perceptual suppression in amblyopia. *Front Hum Neurosci* 2022;16:949395.
- 2 Ip IB, Emir UE, Lunghi C, *et al.* GABAergic inhibition in the human visual cortex relates to eye dominance. *Sci Rep* 2021;11(1):17022.
- 3 Cisneros-Franco JM, Voss P, Thomas ME, et al. Critical periods of brain development. Handb Clin Neurol 2020;173:75-88.
- 4 Severin D, Hong SZ, Roh SE, et al. All-or-none disconnection of pyramidal inputs onto parvalbumin-positive interneurons gates ocular dominance plasticity. Proc Natl Acad Sci U S A 2021;118(37):e2105388118.

- 5 Lu KQ, Hong Y, Tao MD, et al. Depressive patient-derived GABA interneurons reveal abnormal neural activity associated with HTR2C. EMBO Mol Med 2023;15(1):e16364.
- 6 Rezaei S, Prévot TD, Vieira E, et al. LPS-induced inflammation reduces GABAergic interneuron markers and brain-derived neurotrophic factor in mouse prefrontal cortex and hippocampus. Brain Behav Immun Health 2024;38:100761.
- 7 Matsuda YT, Miyamoto H, Joho RH, *et al.* Kv3.1 channels regulate the rate of critical period plasticity. *Neurosci Res* 2021;167:3-10.
- 8 Xie LQ, Zhao KX. Research progress on the synaptic mechanism of amblyopia. *Chin J Ophthalmol* 2008; 44(11):1045-1049.
- 9 Tansley S, Gu N, Guzmán AU, et al. Microglia-mediated degradation of perineuronal nets promotes pain. Science 2022;377(6601):80-86.
- 10 Fawcett JW, Fyhn M, Jendelova P, *et al*. The extracellular matrix and perineuronal nets in memory. *Mol Psychiatry* 2022;27(8):3192-3203.
- 11 Aronitz EM, Kamermans BA, Duffy KR. Development of parvalbumin neurons and perineuronal nets in the visual cortex of normal and dark-exposed cats. *J Comp Neurol* 2021;529(11):2827-2841.
- 12 Xie LQ, Xu GX, Zhang J, *et al*. The postnatal development of perineuronal net, Nogo receptor and the effect of fluoxetine on remodeling it in the visual cortex of rats. *Zhonghua Yan Ke Za Zhi* 2019;55(1):37-45.
- 13 Galán-Llario M, Rodríguez-Zapata M, Fontán-Baselga T, et al. Pleiotrophin overexpression reduces adolescent ethanol consumption and modulates ethanol-induced glial responses and changes in the perineuronal nets in the mouse hippocampus. CNS Neurosci Ther 2024;30(12):e70159.
- 14 Xie LQ, Xu GX, Ni Y, *et al*. The effects of fluoxetine and its machanism on the restores of visual cortex plasticity in the adult rats by visual electrophysiological research. *Chin J Exp Ophthalmol* 2016;34:965-970.
- 15 Carulli D, Verhaagen J. An extracellular perspective on CNS maturation: perineuronal nets and the control of plasticity. *Int J Mol Sci* 2021;22(5):2434.
- 16 Belliveau C, Théberge S, Netto S, et al. Chondroitin sulfate glycan sulfation patterns influence histochemical labeling of perineuronal nets: a comparative study of interregional distribution in human and mouse brain. Glycobiology 2024;34(8):ewae049.
- 17 Li XH, Ren DY, Luo B, *et al.* Perineuronal nets alterations contribute to stress-induced anxiety-like behavior. *Mol Neurobiol* 2024;61(1):411-422.
- 18 Gao FL, Liu G, Qiao YS, et al. Streptavidin-conjugated DNA for the

- boronate affinity-based detection of poly(ADP-ribose) polymerase-1 with improved sensitivity. *Biosensors* 2023;13(7):723.
- 19 Alonge KM, Herbert MJ, Yagi M, *et al.* Changes in brain matrix glycan sulfation associate with reactive gliosis and motor coordination in mice with head trauma. *Front Behav Neurosci* 2021;15:745288.
- 20 Testa D, Prochiantz A, di Nardo AA. Perineuronal nets in brain physiology and disease. *Semin Cell Dev Biol* 2019;89:125-135.
- 21 Liang X, Tang J, Qi YQ, *et al.* Exercise more efficiently regulates the maturation of newborn neurons and synaptic plasticity than fluoxetine in a CUS-induced depression mouse model. *Exp Neurol* 2022;354:114103.
- 22 Wei NL, Li C, Zhu YL, *et al.* Fluoxetine regulates the neuronal differentiation of neural stem cells transplanted into rat brains after stroke by increasing the 5HT level. *Neurosci Lett* 2022;772:136447.
- 23 Fefeu M, Blatzer M, Kneppers A, et al. Serotonin reuptake inhibitors improve muscle stem cell function and muscle regeneration in male mice. Nat Commun 2024;15(1):6457.
- 24 Gan HY, Zhang Q, Zhu B, et al. Fluoxetine reverses brain radiation and temozolomide-induced anxiety and spatial learning and memory defect in mice. J Neurophysiol 2019;121(1):298-305.
- 25 Karpova NN, Pickenhagen A, Lindholm J, et al. Fear erasure in mice requires synergy between antidepressant drugs and extinction training. *Science* 2011;334(6063):1731-1734.
- 26 Ohira K, Hagihara H, Miwa M, et al. Fluoxetine-induced dematuration of hippocampal neurons and adult cortical neurogenesis in the common marmoset. Mol Brain 2019;12(1):69.
- 27 Levy MJF, Boulle F, Emerit MB, *et al.* 5-HTT independent effects of fluoxetine on neuroplasticity. *Sci Rep* 2019;9(1):6311.
- 28 Ohira K, Miyakawa T. Chronic treatment with fluoxetine for more than 6 weeks decreases neurogenesis in the subventricular zone of adult mice. *Mol Brain* 2011;4:10.
- 29 Liu H, Xu HW, Yu T, *et al.* Expression of perineuronal nets, parvalbumin and protein tyrosine phosphatase σ in the rat visual cortex during development and after BFD. *Curr Eye Res* 2013;38(10):1083-1094.
- 30 Gong L, Reynaud A, Hess RF, et al. The suppressive basis of ocular dominance changes induced by short-term monocular deprivation in normal and amblyopic adults. *Invest Ophthalmol Vis Sci* 2023;64(13):2.
- 31 Ohira K, Takeuchi R, Iwanaga T, et al. Chronic fluoxetine treatment reduces parvalbumin expression and perineuronal nets in gammaaminobutyric acidergic interneurons of the frontal cortex in adult mice. Mol Brain 2013;6:43.